H), 1.15 (d, J = 7, 3 H), 1.16 (s, 3 H), 1.19 (s, 3 H), 1.19 (t, J = 7, 3 H), 3.28 (sept, J = 7, 1 H), 3.51 (q, J = 7, 2 H), 3.83 (d, J = 12, 1 H), 4.56 (s, 1 H), 4.65 (d, J = 12, 1 H), and in DMSO-d_6 δ 1.01 (d, J = 7, 3 H), 1.06 (d, J = 7, 3 H), 1.11 (d, J = 7, 3 H), 1.12 (s, 3 H), 1.13 (s, 3 H), 3.34 (sept, J = 7, 1 H), 3.42 (q, J = 7, 2 H), 3.96 (d, J = 11, 1 H), 4.41 (d, J = 11, 1 H), 4.48 (s, 1 H). Upon addition of D_2O to the sample in DMSO-d_6, some of **17** was converted to 5,5-dimethyl-4-isopropyl-3-hydroxy-2-oxomorpholine (**21**), as indicated by comparison of the ^1H NMR spectral patterns with those described for **21** above.

Acknowledgment. Financial support from the NSF in the form of Grant CHE-8903637 and from the University of Colorado Council on Research and Creative Work in the form of a Faculty Fellowship to T.H.K. are gratefully acknowledged. We thank Giorgio Gaudiano for many helpful discussions.

Registry No. 8, 136476-52-3; **9**, 136476-53-4; **10**, 136476-54-5; **12**, 136503-80-5; **13**, 136503-81-6; **17**, 136476-61-4; **18**, 136476-60-3; **19**, 136476-59-0; **20**, 136476-57-8; **21**, 136476-58-9; **22**, 136476-55-6; **23**, 136476-56-7; *dl*-TM-3′ dimer, 136476-50-1; *meso*-TM-3′ dimer, 136476-51-2; *meso*-DEM-3 dimer, 136476-49-8; *dl*-DIM-3 dimer, 136476-48-7; *meso*-DIM-3 dimer, 136476-47-6; *dl*-DIM-3 peroxide, 136476-46-5; *meso*-DIM-3 peroxide, 136476-45-4; *dl*-DEM-3 peroxide, 136476-44-3; *meso*-DEM-3 peroxide, 136503-79-2; DPPH, 1898-66-4; 2-(methylamino)-2-methylpropanol, 27646-80-6; 2-amino-2-methylpropanol, 124-68-5; 2-(((*tert*-butyloxy)carbonyl)amino)-2-methylpropanol, 102520-97-8; 2-(ethylamino)-2-methylpropanol, 82922-13-2; 2-(isopropylamino)-2-methylpropanol, 90434-44-9.

Supplementary Material Available: A complete description of the X-ray crystallographic determinations of *dl*-TM-3′, *meso*-DEM-3, and *meso*-DIM-3 dimers, including tables of atomic coordinates, isotropic and anisotropic displacement parameters, bond lengths, and bond and torsion angles (26 pages); listing of observed and calculated structure factors (17 pages). Ordering information is given on any current masthead page.

Photophysical Properties of C_{70}

James W. Arbogast and Christopher S. Foote*

Contribution from the Department of Chemistry and Biochemistry, University of California—Los Angeles, Los Angeles, California 90024. *Received May 22, 1991. Revised Manuscript Received July 8, 1991*

Abstract: Several important photophysical properties of the fullerene C_{70} have been determined. Fluorescence is weak but measurable. The yields of triplet C_{70} and of singlet oxygen are high, but not quite quantitative; the triplet energy is slightly above 33 kcal/mol. The triplet has an absorption spectrum that resembles that of C_{60} in some respects but is somewhat stronger and lacks a strong red-infrared absorption present in the C_{60} spectrum. Overall, the behavior of C_{70} is similar to that of C_{60}, but the lower symmetry relaxes the forbiddenness of some absorption and emission processes.

Introduction

Preparation and purification of the surprisingly stable spheroidal carbon molecules ("fullerenes") C_{60} and C_{70}[1-5] have created a massive effort to determine the properties of these new molecules.[6-10] We have reported many photophysical properties of C_{60},[6] some of which have recently been confirmed.[7,8] In particular, C_{60} gives a nearly quantitative yield of triplet and singlet oxygen. We now report that C_{70} has photophysical properties that resemble those of C_{60} but differ in important respects.

Experimental Section

Materials. Benzene (Fisher Spectranalyzed) was purified by washing with H_2SO_4, followed by distillation from LAH. Benzonitrile (Eastman) was purified by washing with K_2CO_3, followed by distillation from P_2O_5. Deuterated benzene (Cambridge Isotope Laboratories), hexanes (Fisher Spectranalyzed), 3-methylpentane (Aldrich), and methylcyclohexane (Aldrich Gold Label) were used as received. Anthracene (MC&B) was purified by recrystallization from acetone, and acridine (Aldrich) from toluene. Tetraphenylporphine (TPP), rubrene (Aldrich), and tetracene (Aldrich) were used as received. C_{60} and C_{70} were prepared and purified by the previously reported method.[5,9]

Steady-State Spectroscopy. Steady-state emission spectra were recorded on a SPEX Fluorolog 2 fluorimeter, equipped with a Hamamatsu R928 photomultiplier tube (PMT). All solutions were analyzed in a 1-cm^2 cell, and oxygen was removed by purging with argon (Liquid Air, >99.99% purity) for 25 min when necessary. The approximate fluorescence yield was estimated by comparing the fluorescence intensities of C_{70} and tetracene, with use of identical optical densities at the excitation wavelength (469 nm).

$^1O_2$ Quantum Yields. The apparatus was a modification of the one previously described.[11] C_{70} was excited at 532 and 355 nm by using the second and third harmonic, respectively, of a Quanta-Ray DCR-2 Nd:YAG laser, with pulse energies of 1-3.5 mJ/pulse; the dependence of the signal on energy is linear in this region. The laser pulse was filtered to remove any fundamental with a 355/532 nm pass-1060 nm reflecting mirror (Newport Corp.), followed with a KG-3 (Schott Glass) infrared absorbing filter. The 355-nm pulse was also filtered with a 355 nm

(1) Haufler, R. E.; Conceicao, J.; Chibante, L. P. F.; Chai, Y.; Byrne, N. E.; Flanagan, S.; Haley, M. M.; O'Brien, S. C.; Pan, C.; Xiao, Z.; Billups, W. E.; Ciufolini, M. A.; Hauge, R. H.; Margrave, J. L.; Wilson, L. J.; Curl, R. F.; Smalley, R. E. *J. Phys. Chem.* **1990**, *94*, 8634-8636.
(2) Krätschmer, W.; Fostiropoulos, K.; Huffman, D. R. *Chem. Phys. Lett.* **1990**, *170*, 167-170.
(3) Krätschmer, W.; Lamb, L. D.; Fostiropoulos, K.; Huffman, D. R. *Nature* **1990**, *347*, 354-358.
(4) Taylor, R.; Hare, J. P.; Abdul-Sada, A. K.; Kroto, H. W. *J. Chem. Soc., Chem. Commun.* **1990**, 1423-1425.
(5) Ajie, H.; Alvarez, M. M.; Anz, S. A.; Beck, R. D.; Diederich, F.; Fostiropoulos, K.; Huffman, D. R.; Krätschmer, W.; Rubin, Y.; Schriver, K. E.; Sensharma, D.; Whetten, R. L. *J. Phys. Chem.* **1990**, *94*, 8630-8633.
(6) Arbogast, J. W.; Darmanyan, A. O.; Foote, C. S.; Rubin, Y.; Diederich, F. N.; Alvarez, M. M.; Anz, S. J.; Whetten, R. L. *J. Phys. Chem.* **1991**, *95*, 11-12.
(7) Wasielewski, M. R.; O'Neil, M. P.; Lykke, K. R.; Pellin, M. J.; Gruen, D. M. *J. Am. Chem. Soc.* **1991**, *113*, 2774-2776.
(8) Haufler, R. E.; Wang, L.-S.; Chibante, L. P. F.; Changming, J.; Conceicao, J. J.; Chai, Y.; Smalley, R. E. *Chem. Phys. Lett.*, in press.
(9) Allemand, P.-M.; Koch, A.; Wudl, F.; Rubin, Y.; Diederich, F.; Alvarez, M. M.; Anz, S. J.; Whetten, R. L. *J. Am. Chem. Soc.* **1990**, *113*, 1050-1051.
(10) Diederich, F. N.; Whetten, R. L. *Angew. Chem., Int. Ed. Engl.*, in press.
(11) Ogilby, P. R.; Foote, C. S. *J. Am. Chem. Soc.* **1982**, *104*, 2069-2070.

0002-7863/91/1513-8886$02.50/0

Table I. Photophysical Properties of C_{70}

property	value[a]
E_S	44.1 kcal/mol[b]
E_T	33.0 kcal/mol ≤ E_T < 42 kcal/mol[c]
ϵ_T (400 nm)	$(1.4 \pm 0.1) \times 10^4$ M^{-1} cm^{-1}
τ_T	130 ± 10 μs[d]
k_O	$(9.4 \pm 1.5) \times 10^8$ M^{-1} s^{-1}
$\Phi_{^1O_2}$ (355 nm)	0.81 ± 0.15[e]
Φ_T (355 nm)	0.9 ± 0.15[f]
S_Δ (355 nm)	~1.0 ± 0.2[g]
$\Phi_{^1O_2}$ (532 nm)	0.81 ± 0.15[h]
$k_q(^1O_2)$	not measurable[i]

[a] All measurements in C_6H_6 or C_6D_6 were taken at room temperature; $[C_{70}] \approx 1 \times 10^{-5}$ and 4×10^{-5} M (OD ≈ 0.3) at λ_{exc} 355 and 532 nm, respectively, unless otherwise noted. [b] Calculated from the presumed 0–0 band at 648 nm (see text). [c] See text. [d] In argon-degassed solution. [e] Average of five determinations at varied laser energies (1–3 mJ/pulse); OD = 0.3–0.5, with TPP ($\Phi_\Delta = 0.62$)[20] as standard in air-saturated C_6H_6. [f] Measured by comparison of the benzophenone T–T absorption and C_{70} T–T absorption under the same conditions (see the Experimental Section). [g] Probability of $^1O_2$ formation from triplet under conditions of complete oxygen quenching; $\Phi_{^1O_2} = (\Phi_T)(S_\Delta)$. [h] Average of seven determinations, same conditions as for $\Phi_{^1O_2}$ (355 nm). [i] No change in $^1O_2$ lifetime on adding C_{70} up to 4.9×10^{-4} M (see the Experimental Section).

pass–532 nm reflecting mirror. The near-infrared emission from $^1O_2$ was monitored at right angles to the laser beam and filtered with RG-850 (Schott Glass) and silicon 1100-nm (Infrared Optics) cutoff filters. The detector was a 2-mm (C_6H_6) or 5-mm (C_6D_6) germanium diode (Opto-Electronics) with a preamplifier (OP-37, Analog Devices) operating in a transimpedance mode, with a 500-KΩ feedback resistor followed by a Comlinear CLC E220 amplifier. The signal was averaged (15–25 shots) in a transient digitizer (Analogic Data 6000) and then transferred to a Macintosh IIci computer by using Labview software. Quantum yields of singlet oxygen formation were determined by extrapolation of emission intensities to zero time as defined by the trigger pulse of a photodiode (MRD510) monitoring laser scatter from the Pellin-Broca prism of the harmonic separator. The intensities at time zero were corrected to 100% absorption (from absorbances varying from 0.3 to 0.8) and compared to the singlet oxygen quantum yield of TPP under air, corrected in the same way.

Singlet oxygen quenching by C_{70} was measured in C_6D_6 under air, with excitation at 532 nm. TPP was used as the singlet oxygen sensitizer ($OD_{532\,nm}$ = 0.46 at zero C_{70} concentration). Added C_{70} caused no decrease in the lifetime of $^1O_2$ at concentrations up to 4.9×10^{-4} M.

Time-Resolved Spectroscopy. The spectra and decay kinetics of transient intermediates were measured with a time resolution ≤100 ns. The solutions were excited by a Quanta-Ray DCR-2 Nd:YAG laser (3–20 mJ/pulse) at 355 and 532 nm. A Hanovia 100-W xenon lamp was used for the probe beam, which was passed through a Jarrell-Ash Model 82-410 monochromator (1-mm slits) and detected with a Hamamatsu R928 PMT. The output from the PMT was monitored with a LeCroy 9410 waveform recorder coupled with a Macintosh IIci computer using Labview software. Kinetic curves were averaged over 20–50 laser pulses.

The differential extinction coefficient of triplet C_{70} at 400 nm ($\epsilon_T - \epsilon_0$, where ϵ_T and ϵ_0 are the extinction coefficients of the triplet and ground states, respectively) was obtained by energy transfer to rubrene. The optical density (OD) of triplet C_{70} produced with an Nd-YAG laser pulse at 355 nm in argon-saturated C_6H_6 was measured at 400 nm. Rubrene was then added at a concentration (8×10^{-5}) sufficient to give 96% quenching of $^3C_{70}$. Excitation at 355 nm gives triplet rubrene solely by energy transfer, since rubrene absorbs only slightly at this wavelength (OD ~0.05 vs 0.85 for C_{70}). Therefore, the amount of triplet produced is approximately the same for both C_{70} and rubrene. The OD of triplet rubrene was measured at 505 nm, where $^3C_{70}$ has no absorption (see Figure 2), and corrected to 100% quenching of $^3C_{70}$. The value ($\epsilon_T^{Rub} - \epsilon_0^{Rub}$) used for rubrene at λ_{max} is 1.76×10^4 M^{-1} cm^{-1}.[12] The triplet extinction coefficient ϵ_T was then calculated from the following equation:

$$\epsilon_T^{C_{70}} = \frac{(\epsilon_T^{Rub} - \epsilon_0^{Rub})OD_T^{C_{70}}}{OD_T^{Rub}} + \epsilon_0^{C_{70}}$$

The triplet extinction coefficient determined in the above way was used to determine the triplet quantum yield (Φ_T) at 355 nm by comparison with benzophenone (bp). Excitation of separate samples of C_{70} and benzophenone with equal laser energy and equal $OD_{355\,nm}$ yields data from which Φ_T was determined by the following equation:

$$\Phi_T^{C_{70}} = \frac{(\Delta OD_T^{C_{70}})(\epsilon_T^{bp} - \epsilon_0^{bp})(\Phi_T^{bp})}{(\Delta OD_T^{bp})(\epsilon_T^{C_{70}} - \epsilon_0^{C_{70}})}$$

where ΔOD_T is the absorbance of the triplet. Using $\Phi_T = 1.0$ and $\epsilon_T = 7220$ M^{-1} cm^{-1} at 530 nm for benzophenone in benzene,[13] we measured the optical density of triplet benzophenone at 530 nm and C_{60} at 400 nm (both in C_6H_6) to determine Φ_T for C_{70} (Table I).

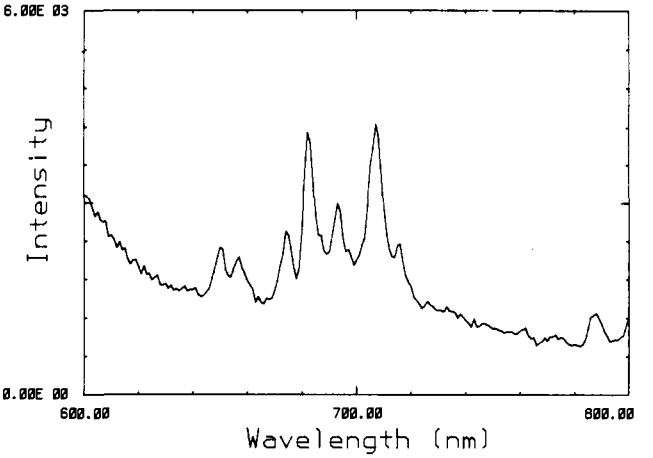

Figure 1. C_{70} fluorescence at 77 K in a methylcyclohexane/3-methylpentane (3:1) glass.

Results

The absorption spectra of C_{60} and C_{70} have been published.[5] The spectra for the two compounds are rather similar, except that the visible absorption of C_{70} is markedly stronger than that of C_{60}, probably because its lower symmetry relaxes the forbiddenness of the longest wavelength transition. The physical processes of interest are summarized in the scheme below, where k_1 is the triplet–triplet energy transfer rate constant and k_O is the rate constant of energy transfer to oxygen.

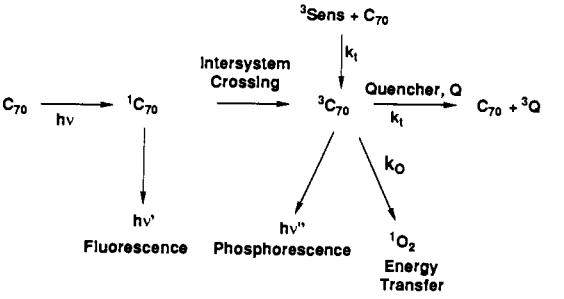

In contrast to C_{60}, for which neither fluorescence nor phosphorescence could be detected, very weak fluorescence from C_{70} was detected at room temperature in both hexane (UV excitation) and benzene (visible excitation), and also at 77 K in a methylcyclohexane 3-methylpentane (3:1) glass. Broad emission between 650 and 725 nm at room temperature (not shown) sharpens at 77 K, yielding a highly structured spectrum with λ_{max} 682 nm (Figure 1). Because of the weakness of the emission, there is considerable solvent background reflected by the rising base line at 600 nm. The emission peaks are at 650, 657, 674, 682, 693, 707, and 716 nm, corresponding to vibrational spacings of 164, 384, 174, 233, 286, and 178 cm^{-1}, respectively. The zero–zero transition presumably lies near 648 nm between the longest wavelength absorbance at 646 nm[5] and the shortest wavelength observed fluorescence at 650 nm, corresponding to a singlet energy (E_S) of 44.1 kcal/mol. The fluorescence is very weak; its yield is ~8.5×10^{-4} as determined by comparison with the tetracene fluorescence at 540 nm using $\Phi_F = 0.21$ for tetracene.[14] Since

(12) Darmanyan, A. P. *Izv. Akad. Nauk SSSR* **1982**, *8*, 1888–1891.

(13) Hurley, J. K.; Sinai, N.; Linschitz, H. *Energ. Res. Abstr.* **1983**, *8*(8), Abstr. No. 18360.

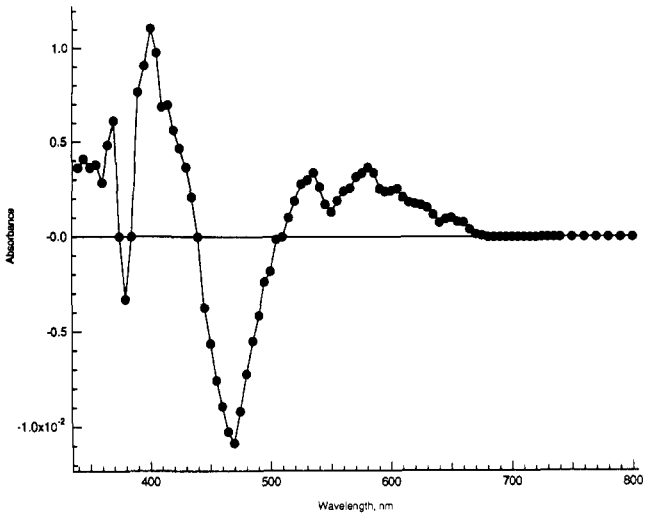

Figure 2. Differential triplet–triplet absorption spectrum of C_{70} in benzene.

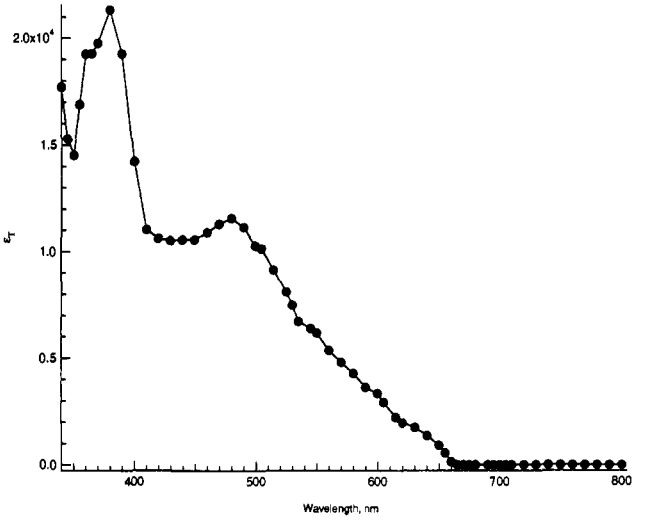

Figure 3. Corrected triplet–triplet absorption spectrum of C_{70} in benzene.

intensities rather than integrated spectra were compared, this value is only a rough estimate.

The fluorescence excitation spectrum of C_{70} does not completely mimic the absorption spectrum. The absorption peak at 468 nm and, to a lesser extent, that at 377 nm are major sources of the fluorescence, but the shorter wavelength absorptions do not produce detectable emission at 682 nm (data not shown). Upper singlet excited states of C_{70} apparently do not produce S_1 efficiently. Because of the weakness of the emission, we cannot rule out the possibility that it results from an impurity.

Phosphorescence of C_{60} has not yet been observed[6,7] despite the high triplet yield. However, Wasielewski et al.[7] measured C_{70} phosphorescence between 790 and 890 nm at 77 K. We therefore made no effort to study the phosphorescence.

The triplet–triplet absorption spectrum for C_{70} is given in Figure 2 and shows large negative peaks caused by depletion of the ground state.

The differential extinction coefficient at 400 nm ($\epsilon_T - \epsilon_{S0}$), 3.1 $\times$ 10^3 M^{-1} cm^{-1}, was estimated by the method of Bensasson and Land[15] with use of energy transfer to give the rubrene triplet, whose T–T extinction is known (see the Experimental Section). The corrected absorption spectrum (ϵ_T vs λ) for C_{70} was prepared by correcting for ground-state depletion (by adding ϵ_{S0}) at each wavelength and is shown in Figure 3. This spectrum is quite

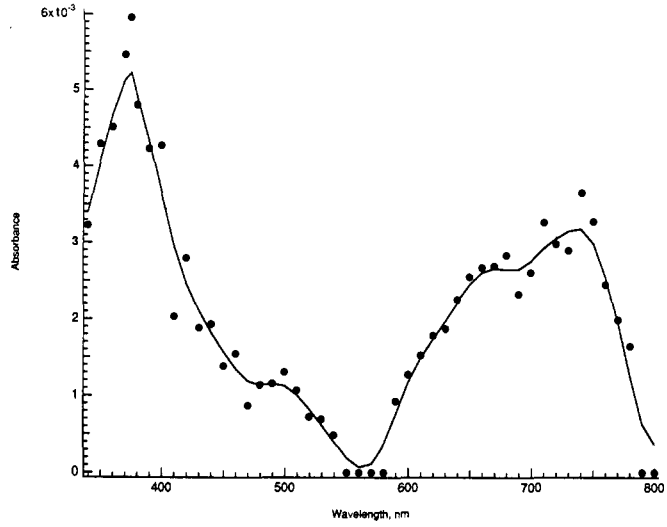

Figure 4. Triplet–triplet absorption spectrum of C_{60} in benzonitrile (λ_{exc} = 420 nm). The solid line is a smooth curve through the points.

similar to the ground-state absorption spectrum.

The triplet–triplet absorption spectrum for C_{60} has now also been detected over a much wider region than originally reported[6] and is shown in Figure 4 for completeness. There is a large absorption feature in the 600–800-nm region that could not be observed with our previous detector.

The triplet lifetime of C_{70} is 130 $\pm$ 10 μs with a sample of low concentration (OD_{355} = 0.29) and a laser energy of 1–2 mJ/pulse. Under these conditions, triplet–triplet annihilation is negligible, as evidenced by a good first-order exponential fit to the data over the entire decay curve (data not shown). Triplet lifetimes previously published by Wasielewski et al. at 9 K in a glass (C_{60} = 0.29–0.41 ms, C_{70} = 51 ms)[7] and by Haufler et al. in a supersonic (and supercooled) molecular beam (C_{60} = 42 μs, C_{70} = 41 μs)[8] indicate that, as expected, the lifetimes depend greatly on measurement conditions. The triplet state of C_{70} is efficiently quenched by $^3O_2$; in air-saturated C_6H_6 the lifetime is 730 $\pm$ 50 ns. With the oxygen concentration in air-saturated benzene of 1.45 $\times$ 10^{-3} M, this value yields a rate constant for quenching by oxygen of k_Q = 9.4 $\times$ 10^8 M^{-1} s^{-1}, which is slightly lower than for C_{60}.

The energy level of $^3C_{70}$ (E_T) has been determined to be 35.3 kcal/mol by phosphorescence in a glass at 77 K[7] and ~37 kcal/mol by resonance two-photon ionization spectroscopy in the gas phase.[8] We estimated the energy by triplet–triplet energy transfer. C_{70} quenches the triplet states of both acridine (E_T = 45.3 kcal/mol)[16] and anthracene (E_T = 42 kcal/mol)[16] efficiently, with rate constants of (8.1 $\pm$ 0.3) $\times$ 10^9 M^{-1} s^{-1} and (6.2 $\pm$ 0.6) $\times$ 10^9 M^{-1} s^{-1}, respectively. The rate of quenching of the triplet state of TPP (E_T = 33.0 kcal/mol)[17] by C_{70} is significantly lower, k_q = (4.4 $\pm$ 1.5) $\times$ 10^7 M^{-1} s^{-1}. The rate of energy transfer from C_{70} triplet to produce the tetracene triplet (E_T = 29.3 kcal/mol)[18] is (2.3 $\pm$ 0.4) $\times$ 10^9 M^{-1} s^{-1}, slightly but significantly below the diffusion-controlled value. Thus, we conclude that, as with C_{60}, the energy level of the triplet state of C_{70} lies near TPP and well below anthracene, i.e., 33.0 kcal/mol $\leq$ E_T < 42 kcal/mol.

Determination of the rate of the reverse quenching of $^3C_{70}$ by TPP would be very useful in determining the exact triplet energy, but the overlap of the triplet–triplet absorption spectra make this measurement virtually impossible under our experimental conditions. It is well known[19] that the rate of triplet energy transfer depends on the relative triplet energies; when the triplet energy

(14) Berlman, I. B. *Handbook of Fluorescence Spectra of Aromatic Molecules*; Academic Press: New York, 1965.
(15) Bensasson, R.; Land, E. J. *Trans. Faraday Soc.* **1971**, *67*, 1904–1915.
(16) Birks, J. B. *Photophysics of Aromatic Molecules*; Wiley-Interscience: New York, 1970.
(17) McLean, A. J.; McGarvey, D. J.; Truscott, T. G.; Lambert, C. R.; Land, E. J. *J. Chem. Soc., Faraday Trans.* **1990**, *86*, 3075–3080.
(18) McGlynn, S.; Padahye, M.; Kasha, M. *J. Chem. Phys.* **1955**, *23*, 593–595.
(19) Lamola, A. A.; Turro, N. J. *Techniques of Organic Chemistry: Energy Transfer and Organic Photochemistry*; Leermakers, P. A., Weissberger, A., Eds.; Interscience Publishers: New York, 1969; pp 44–50.

of the donor is 0–2 kcal/mol below that of the acceptor, the rate constant is more than 2 orders of magnitude below the diffusion-controlled value. Thus, the observed rate of energy transfer from ^{3}TPP to C_{70} would be expected if the C_{70} triplet energy is 33–35 kcal/mol, in excellent agreement with the value of Wasielewski et al.[7]

C_{70}, like C_{60},[6] produces singlet oxygen in large quantities, as measured by $^1O_2$ luminescence at 1268 nm.[11] The quantum yield ($\Phi_{^1O_2}$) is 0.81 ± 0.15 when excited at both 355 and 532 nm. Since $^1O_2$ is formed by energy transfer from the highly populated C_{70} triplet state to molecular oxygen, these values also represent a lower limit for the quantum yield of triplet production (Φ_T). In excellent agreement with this conclusion, the value for Φ_T at 355 nm, as determined by comparison with benzophenone (see Experimental Section), were in the range 0.9 ± 0.15 in four separate experiments. Thus S_Δ, the efficiency of formation of $^1O_2$ from the triplet, is 1.0 within experimental error.

We were unable to detect $^1O_2$ quenching by C_{70} in C_6D_6. Marginal quenching was detected with C_{60},[6] the mechanism of which is presently unknown, but solubility limitations precluded measurements at high enough concentration to detect any quenching by C_{70}, even of the magnitude seen with C_{60}. As with C_{60}, however, no destruction of starting material or formation of new products (by UV–visible absorption spectra and HPLC) occurs under O_2, following hundreds of laser pulses at either excitation wavelength or with broad-band excitation with a powerful lamp for many hours.

Discussion

Because of the reduced symmetry of C_{70} relative to C_{60}, the $S_0 \rightarrow S_1$* transition is not as strongly forbidden, and the visible maxima are much stronger. This lowered forbiddenness also accounts for the fact that weak fluorescence from this transition can be observed in C_{70}, in contrast to C_{60}. Increased triplet–triplet absorption coefficients (roughly 1.5 times that of C_{60}) may be caused by the same factor.

As with C_{60}, the small S–T splitting in C_{70} ($\Delta E_{S_1\text{-}T} \approx 9$ kcal/mol) is probably a result of the large diameter of the molecule and the resulting small electron–electron repulsion energy.[21] This small splitting, the probable low value of the fluorescence rate constant (from the low extinction coefficient), and the expected large spin–orbital interaction in the spheroidal C_{70} explains why intersystem crossing (ISC) is a dominant process. Wasielewski has measured the rates of intersystem crossing ($C_{60} = 3.0 \times 10^{10}$ s^{-1} and $C_{70} = 8.7 \times 10^9$ s^{-1}). The larger diameter and resulting lower curvature of C_{70} than C_{60} would predict a smaller spin–orbit coupling and provide a rationale for the lower intersystem crossing rate constant and somewhat lower triplet production efficiency in C_{70}.

The singlet oxygen quantum yields at 532 and 355 nm, while high, are slightly lower than unity. With C_{60}, the yield is 0.74 at 355 nm, but 1.0 at 532 nm.[6] The lower yield for C_{70} at 532 nm, in comparison with C_{60}, must result from minor pathways for deactivation of $^1C_{70}$ other than intersystem crossing, for instance, internal conversion.

The very high singlet oxygen yield and inertness to destruction of C_{70} suggests potential for photodynamic damage to biological systems, as with C_{60}.[6] Experiments to test this suggestion are in progress.

Acknowledgment. This work was supported by NSF Grant No. CHE89-11916 and NIH Grant No. GM-20080. We thank F. Ettl, F. Diederich, and R. Whetten for C_{70} and C_{60} and A. Darmanyan for helpful discussion.

Note Added in Proof. A recent letter[22] suggests that C_{60} and C_{70} are unstable to light. We have exposed solutions of each in benzene to unfiltered light from a 300-W xenon lamp for many hours under O_2 without observable degradation (UV–vis and HPLC). Also, solutions of both compounds were allowed to stand in a California window exposed to full skylight for 9 days; C_{60} was unchanged, while C_{70} showed <1% formation of an unidentified new product by HPLC.[23] We concur that samples on some batches of alumina and on other adsorbents have variable stability, with C_{70} being lost more readily than C_{60}, but we do not believe that light is an important contributor to this destruction.

Registry No. C_{60}, 99685-96-8; C_{70}, 135105-58-7; rubrene, 517-51-1; oxygen, 7782-44-7.

(20) Schmidt, R.; Afshari, E. *J. Phys. Chem.* **1990**, *94*, 4377–4378.
(21) McGlynn, S. P.; Azumi, T.; Kinoshita, M. *Molecular Spectroscopy of the Triplet State*; Prentice-Hall: Englewood Cliffs, NJ, 1969.
(22) Taylor, R.; Parsons, J. P.; Avent, A. G.; Rannard, S. R.; Dennis, T. J.; Hare, J. P.; Kroto, H. W.; Walton, D. R. M. *Nature* **1991**, *351*, 277.
(23) Ettl, F.; Diederich, F. Personal communication.

Synthesis and Formal [4 + 2] Cycloaddition Reactions of Vinylimido Complexes of Titanocene

Kenneth M. Doxsee,*,† Judah B. Farahi,† and Håkon Hope‡

Contribution from the Department of Chemistry, University of Oregon, Eugene, Oregon 97403, and Department of Chemistry, University of California, Davis, California 95616.
Received December 17, 1990

Abstract: Sources of the methylidene complex of titanocene, $Cp_2Ti{=}CH_2$, react with nitriles in the presence of donor ligands to afford vinylimido titanocene complexes. The vinylimido complexes react readily with ketones, nitriles, and imines, yielding products that retain the elements of the imido ligand. In no case are products of formal [2 + 2] metathesis obtained. Concerted or stepwise [4 + 2] cycloadditions are suggested as possible mechanisms for these coupling reactions.

Metal–ligand multiply bonded species play a myriad of diverse roles in inorganic and organometallic chemistry.[1] Reports of such complexes as intermediates and isolated species continue to grow in number at a rapid rate. As more and more data are obtained, it becomes possible to formulate generalizations about the reactivity of these species with various classes of organic substrates. Imido complexes of both early and late transition metals, for example, react with aldehydes and ketones in metathesis-type

† University of Oregon.
‡ University of California.

(1) Nugent, W. A.; Mayer, J. M. *Metal-Ligand Multiple Bonds*; Wiley-Interscience: New York, 1988.

0002-7863/91/1513-8889$02.50/0